

Full methylation of H3K27 by PRC2 is dispensable for initial embryoid body formation but required to maintain differentiated cell identity

Sara A. Miller^{1,2}, Manashree Damle¹, Jongmin Kim^{1,2} and Robert E. Kingston^{1,2,*}

ABSTRACT

Polycomb repressive complex 2 (PRC2) catalyzes methylation of histone H3 on lysine 27 and is required for normal development of complex eukaryotes. The nature of that requirement is not clear. H3K27me3 is associated with repressed genes, but the modification is not sufficient to induce repression and, in some instances, is not required. We blocked full methylation of H3K27 with both a small molecule inhibitor, GSK343, and by introducing a point mutation into EZH2, the catalytic subunit of PRC2, in the mouse CJ7 cell line. Cells with substantively decreased H3K27 methylation differentiate into embryoid bodies, which contrasts with EZH2 null cells. PRC2 targets had varied requirements for H3K27me3, with a subset that maintained normal levels of repression in the absence of methylation. The primary cellular phenotype of blocked H3K27 methylation was an inability of altered cells to maintain a differentiated state when challenged. This phenotype was determined by H3K27 methylation in embryonic stem cells through the first 4 days of differentiation. Full H3K27 methylation therefore was not necessary for formation of differentiated cell states during embryoid body formation but was required to maintain a stable differentiated state.

KEY WORDS: PRC2, H3K27 methylation, EZH2, Differentiation, Maintenance, Embryoid body

INTRODUCTION

Polycomb repressive complex 2 (PRC2) is a highly conserved protein complex that is required for proper axial patterning of vertebrates. It comprises the core subunits EZH2, SUZ12, EED and RBAP48 (also known as RBBP4), with additional subunits, some of which are cell-type or developmental stage specific (Healy et al., 2019; Margueron and Reinberg, 2011; Shen et al., 2009; van Mierlo et al., 2019). The complex is crucial for differentiation, but it is not required for the self-renewing phenotype associated with embryonic stem cells (ESCs) (Aloia et al., 2013; Chamberlain et al., 2008). At a molecular level, PRC2 family complexes are the only histone 3 lysine 27 (H3K27) methyltransferases identified in mammals. EZH2 is the primary catalytic component of these complexes, with its paralog EZH1 also contributing to catalytic activity in some instances (Margueron et al., 2008; Shen et al., 2008; Wassef et al., 2019; Xu et al., 2015). Lysine residues can be mono-, di- or

trimethylated, with PRC2 able to catalyze all levels of methylation. Increased methylation is generally associated with gene repression, and H3K27 trimethylation (H3K27me3) is a key marker of facultative heterochromatin. However, the trimethylation of H3K27 is neither required nor sufficient to induce gene repression (Ahmed et al., 2018; Chamberlain et al., 2008; Ferguson et al., 2018; O'Geen et al., 2017). Dissecting the role of trimethylated H3K27 in gene regulation is important for understanding how genes become repressed during development and retain their repression in differentiated cells.

Expression levels of Polycomb complexes have developmental and disease effects. Both hyper-activating and inactivating mutations in PRC2 have been identified from a variety of human cancers (Basheer et al., 2019; Cyrus et al., 2019; Jain and Di Croce, 2016). Malignancies with both types of alterations to PRC2 function have been linked to cancer progression and poor prognosis in a wide variety of tissue (Abdel Raouf et al., 2021; Basheer et al., 2019; Bohm et al., 2019; Bremer et al., 2021; Deng et al., 2019; Dou et al., 2019; Karlowee et al., 2019; Krill et al., 2020; Matsubara et al., 2019; Mechaal et al., 2019; Shi et al., 2019; Tian et al., 2019; Wasenang et al., 2019; Zhang et al., 2019a,b). These findings are consistent with the initial identification of Polycomb-group genes in *Drosophila*, in which haploinsufficiency yielded developmental phenotypes (Lewis and Mislove, 1947; Schuettengruber et al., 2017). Inserting these disease mutations into cells alters the modification profiles of H3K27 and can change their developmental potential. Increased methylation can often push ESCs toward a neuro progenitor phenotype (Juan et al., 2016; Pasini et al., 2007; Thornton et al., 2014). In cancer patients, increased levels of expression of PRC2 components and especially EZH2 leads to hypermethylation and is associated with poor prognosis (Tian et al., 2019; Wu et al., 2019). Consequently, there is significant interest in targeting this complex pharmaceutically. Small molecules that inhibit PRC2 methyltransferase activity have been approved for clinical trials (Fioravanti et al., 2018; Kondo, 2014; Liu et al., 2015; Lue and Amengual, 2018; Qi et al., 2012; Shi et al., 2019; Xu et al., 2015; Yamagishi and Uchimaru, 2017; Yang et al., 2019). It remains, however, unclear how far this activity can be manipulated before risking adverse effects from having too little of the modification present. The ambiguity of the role of H3K27me3 in disease progression increases the importance of understanding the mechanisms by which PRC2 methylation activities regulate gene expression during development.

Previous work on PRC2 has shown that the complex is dispensable for the propagation of self-renewing undifferentiated cells that are phenotypically indistinguishable from wild-type (WT) ESCs. These studies have also shown that PRC2-deficient cells do not differentiate properly (Chamberlain et al., 2008; Lavarone et al., 2019; Pasini et al., 2007, 2004; Shen et al., 2008). As the entire

¹Department of Molecular Biology, Massachusetts General Hospital Research Institute, Massachusetts General Hospital, Boston, MA 02114, USA. ²Department of Genetics, Harvard Medical School, Boston, MA 02115, USA.

*Author for correspondence (kingston@molbio.mgh.harvard.edu)

 R.E.K., 0000-0003-3628-4335

Handling Editor: Haruhiko Koseki
Received 24 August 2020; Accepted 2 March 2021

complex is disrupted when any of the core components are knocked out, it is not clear whether it is solely the lack of methylation that is causing these developmental defects, or whether there are other mechanistic roles PRC2 plays that are distinct from methylation (Collinson et al., 2016; Rai et al., 2013; Shan et al., 2017; Yu et al., 2017). A recent study examined the impacts of mutations in *Ezh2* that block or substantively reduce methylation (Lavarone et al., 2019). When cells blocked for all levels of methylation were differentiated into embryoid bodies (EBs), they showed visual phenotypic differences demonstrating that complete removal of the methyltransferase activity of PRC2 impairs normal differentiation. Substantially reducing methylation with a mutation identical to the one we characterize in this work did not block differentiation to the same extent (Lavarone et al., 2019). Here, we focus on the developmental and molecular phenotypes caused by this latter mutation (R681C) which impacts H3K27me3 but does not remove all methylation activity.

To determine the contribution that H3K27me3 makes to gene repression, we examined cells with the R681C point mutation within the SET domain of *Ezh2*. This is a hypomorph that is substantively defective in trimethylation. We also analyzed cells treated with a small molecule inhibitor that blocks both trimethylation and dimethylation. The expression level of PRC2 has known effects on gene regulation, so we used strategies that do not impact the protein level or complex integrity, thus allowing a focus on methyltransferase activity. There are multiple small molecules that interrupt PRC2 methyltransferase activity both for research and current clinical trials; we used GSK343 (Bradley et al., 2014; Fraigneau et al., 2017; Liu et al., 2015; Xu et al., 2019; Yang et al., 2019). Mutations in the catalytic SET domain of *Ezh2* have been identified from a variety of cancers; we created cell lines containing one of the inactivating mutations for our experiments (Antonyamy et al., 2013). This residue corresponds to *Drosophila* R699, where R699A and R699H mutations have previously been shown to disrupt methyltransferase activity and to alter normal HOX gene expression patterns (Müller et al., 2002). We found that the R681C mutation had a strong impact on H3K27me3 levels, and a lesser impact on H3K27me2 levels in mouse cells. When these cells were differentiated in an undirected fashion, they did not show the significant visual phenotypes seen with *Ezh2* knockout cells. Although expression of some genes was altered, there were a number of PRC2 target genes that did not rely upon H3K27me3 for their regulation. The most dramatic phenotype observed was when cells were challenged to maintain their differentiated identity. Inhibitor-treated and point-mutated cells reverted readily to an ES phenotype when placed back into conditions that support ESC growth. Thus, this hypomorphic mutation that abrogates full methylation of H3K27 impacts the ability of cells to maintain their identity rather than their ability to undergo initial differentiation.

RESULTS

PRC2 catalyzes di- and trimethylation of histone H3 and is associated with gene repression. Previous studies have shown that deletion of PRC2 components in mouse ESCs has minimal effects on the undifferentiated self-renewing state (Juan et al., 2016; Lavarone et al., 2019; Shen et al., 2008; Wassef et al., 2019). Yet deletion of EZH2, the catalytic subunit of PRC2, results in cells that do not differentiate and embryos that are reabsorbed by embryonic day (E)10.5 (O'Carroll et al., 2001). However, the requirements for specific methylation functions of PRC2 in differentiation and in the accompanying changes in gene expression have not been explored in detail. We examined the role for methylation of H3K27 in

regulation by looking at stochastic differentiation of ESCs into EBs. EB formation is a well-studied method of undirected differentiation with predictable changes in gene expression (Fig. 1A; Behringer et al., 2016; Dang et al., 2002). Cells in which PRC2 core components have been deleted fail to form normal EBs, presumably because the cells apoptose when pushed to differentiate (Chamberlain et al., 2008). The precise requirement for the H3K27me3 modification at individual genes during differentiation as well as its role in maintaining cell identity remains unclear.

Inhibiting methyltransferase activity with the small molecule GSK343 does not block differentiation potential

As a starting point to understand the role of H3K27 methylation by PRC2 during ESCs differentiation, we treated cells with the small molecule inhibitor GSK343, which blocks the methyltransferase activity of EZH2 (Fioravanti et al., 2018; Lue and Amengual, 2018; Yang et al., 2019). Treatment with DMSO was used as a control (Fig. 1B). Unlike PRC2 knockouts, GSK343-treated cells form EBs that have a similar morphology to their DMSO-treated counterparts (Fig. 1C). EBs formed after either DMSO or GSK343 treatment are phenotypically similar to those made by WT cells. In contrast, PRC2 knockout cells tested in parallel failed to form EBs (Lavarone et al., 2019; Fig. 2D). Thus, the inhibition of methyltransferase activity can be phenotypically separated from PRC2 knockout cells.

To determine the molecular phenotype of blocking methyltransferase activity, we performed RNA-seq experiments to compare changes in gene expression between cells treated with the inhibitor and control over the differentiation time course. Gene expression was largely similar between the two treatments, especially in early stages of differentiation (Fig. S1). We then examined known PRC2 target genes and found examples of genes for which the expression pattern across differentiation was the same in DMSO- and GSK343-treated cells (e.g. *Tbx3* or *Sox3*; Fig. 1D and Fig. S1C) as well as genes for which expression was altered in GSK343-treated cells (e.g. *Wnt3* and *Itgb7*; Fig. 1D and Fig. S1C). The trends observed with these two classes of genes were found to be mirrored in the full complement of PRC2 targets. We classified PRC2 target genes into two sets, those that required H3K27me3 for their regulation and those that do not need this modification to preserve normal gene expression patterns during EB formation. Genes were defined as independent of the H3K27me3 modification if their expression remained within 1.2-fold of the WT expression at all time points (Fig. 1E,F; Fig. S1E,F). We conclude that inhibiting the methylation activity of PRC2 alters gene expression at a subset of targets but does not block differentiation in the same way that knockouts of the complex do.

Point mutation to the SET domain inhibits methyltransferase activity

We sought to extend and refine the findings made using GSK343 by generating a hypomorphic mutation in *Ezh2* that had a defined impact on H3K27 methylation. We generated mutant cells that allowed us to examine the requirement for full H3K27 trimethylation in gene regulation and differentiation during EB formation. Inactivating point mutations in the SET domain of EZH2 have been identified in several human cancers. Human R635C, which is analogous to mouse R681C, was the residue we selected for analysis in mouse cells. This residue is conserved across species and is located in a region that is important for coordinating the methyl donor (Fig. 2A; Antonyamy et al., 2013; Jiao and Liu, 2015). We purified PRC2 complexes comprising the core components RBAP46/48, EED, SUZ12, EZH2 (WT or mutant)

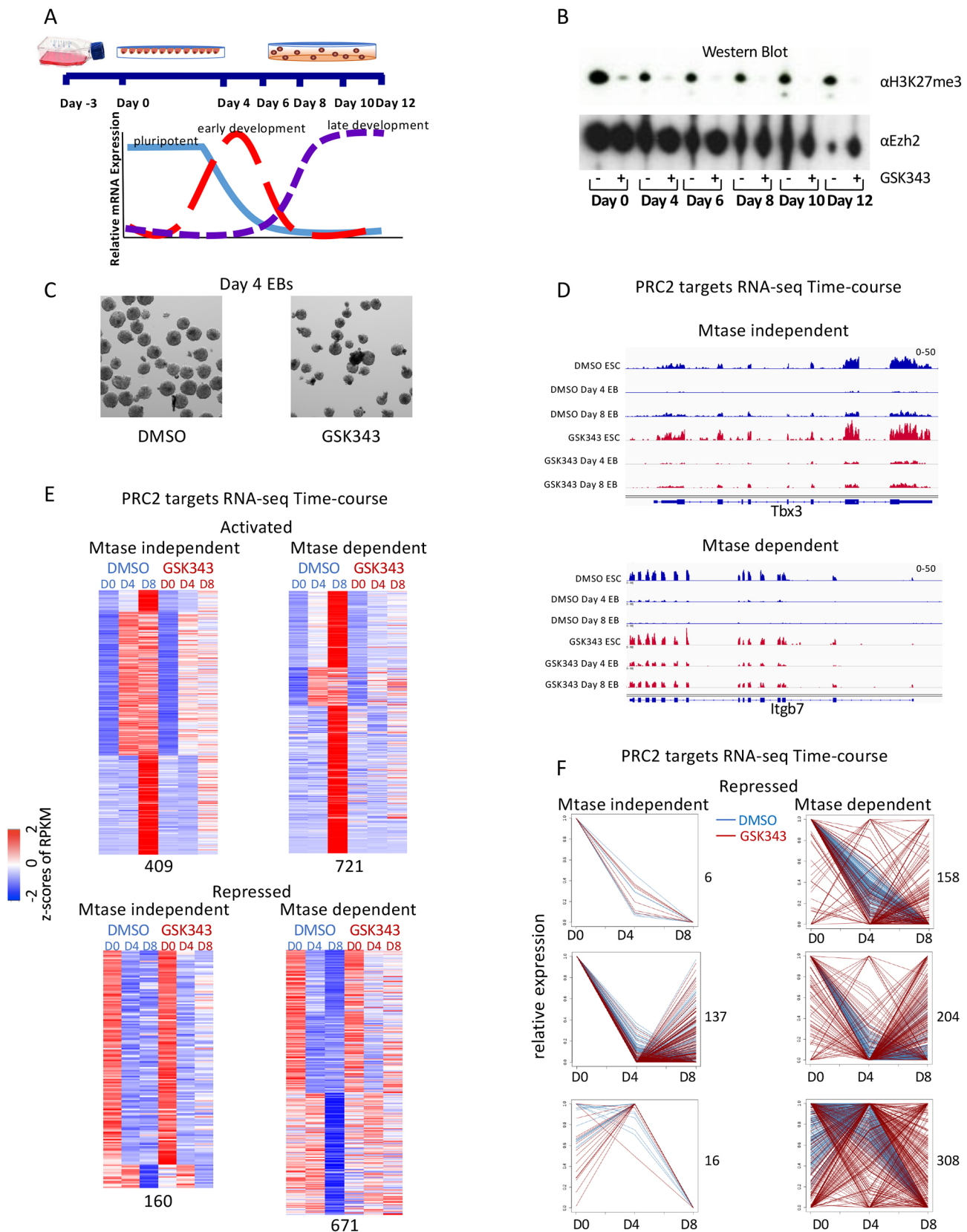


Fig. 1. See next page for legend.

and the accessory protein AEBP2 by pulling down on a flag-tagged SUZ12 (Fig. S2). We confirmed that this residue is important for trimethylation of H3K27 by PRC2 using an *in vitro*

methyltransferase assay. We compared it with WT EZH2 and another SET domain mutation (Y722D) that has been previously shown to block methylation (Lavarone et al., 2019; Fig. 2B). The

Fig. 1. Treatment with EZH2 methyltransferase inhibitor reveals two classes of PRC2 target genes during differentiation. (A) Diagram of embryoid body (EB) formation time course. (B) Western blot of cells treated with GSK343 EZH2 inhibitor or DMSO control probed with H3K27me3 and EZH2 antibodies. (C) Representative image of 54× magnification of day 4 EBs from cells treated with either DMSO control or GSK343. (D) Screen shots from RNA-seq over the EB differentiation time course from methyltransferase (Mtase)-independent (Tbx3) and Mtase-dependent (Itgb7) genes from cells treated with DMSO (blue) or GSK343 (red). (E) Heatmap showing expression patterns of Mtase-dependent and -independent PRC2 target genes in untreated (DMSO) and treated (GSK343) CJ7 cells over development time course. z-Scores of average RPKMs of duplicates are shown for each gene across all samples. Genes are separated based on whether they were activated (top) or repressed (bottom) in untreated cells over time as well as if they had a similar expression pattern in treated cells (Mtase-dependent genes; right) or a different expression pattern (Mtase-independent genes; left). The four groups are further clustered based on fold changes over time in untreated cells. All of the classifications were made based on a 1.5-fold change cutoff in expression levels over time. Numbers of genes in each category are indicated at the bottom. (F) Line diagrams showing relative gene expression of repressed PRC2 target genes from E separated by Mtase-dependent and -independent genes and expression pattern in DMSO-treated cells. Each plot shows all genes from individual clusters from E. Numbers of genes in each cluster are indicated on the right.

complexes that contained WT EZH2 methylated both core histones and purified H3 in a time- and concentration-dependent manner (Fig. S2). In contrast, mutant complexes show drastically reduced levels of activity. Using two separate purifications, residual activity of the mutant complex was always under 2% of the purified WT complexes (Fig. 2B; Fig. S2). We conclude that the *Ezh2* 681C mutation reduces the methyltransferase activity of the complex by at least 98%.

We introduced the R681C mutation into the CJ7 mouse ESC line using the CRISPR-Cas9 system. We isolated two independent clones in the mouse ESC line with this homozygous point mutation in the endogenous *Ezh2* gene (called CJ7 *Ezh2*^{681C-99} and CJ7 *Ezh2*^{681C-102}). The phenotypes that we describe below were consistent between these two independent lines and are consistent with growth phenotypes described recently for the same mutation (Lavarone et al., 2019). The mutant cells look phenotypically similar to WT cells and self-renew (Fig. 2D). This was the anticipated result as knockout cells in the PRC2 core components EZH2 and EED are also phenotypically similar to WT cells and can self-renew. We examined whether the point mutation would lead to significant reduction of H3K27me3 in cells as anticipated from the enzymatic defect seen *in vitro*. Lysine residues can be mono-, di- or trimethylated. Monomethylation is spread broadly throughout the genome and dimethylation is loosely linked with repressed genes, though this is poorly defined in most cell types. Trimethylation of H3K27 is closely associated with repressed genes, presumably owing to binding of the CBX family of proteins contained in the PRC1 complex to K27me3 and subsequent repression by this family of complexes (Bernstein et al., 2006). We performed western blots on whole-cell lysates from WT, knockout and the point-mutant cells and probed them with antibodies to H3K27 di- and trimethylation and EZH2 (Fig. 2C). H3K27me3 was reduced to levels we could not detect in the mutant cells, as was seen in the knockout cells, and levels of dimethylation were lowered, but to a somewhat lesser degree, in the R681C mutant cells. We conclude that in these cells the point mutation substantively reduced trimethylation of H3K27. This is similar to the results found in studies of this and other *Ezh2* point mutations (Lavarone et al., 2019). The R681C mutation therefore offers an opportunity to examine the requirement for trimethylated H3K27 in gene regulation during differentiation.

We examined whether the mutant cell lines would form EBs similar to those formed by WT cells, would apoptose like *Ezh2* or *Eed* knockout cells, or would take an alternate path. We formed EBs by the hanging drop procedure and compared the resultant phenotypes of WT, the point-mutant and knockout cells. We found that the mutant cells formed EBs, making them phenotypically separate from the knockout cells (Fig. 2D). This revealed that the dramatic reduction in H3K27me3 we see in the point-mutant cells does not stop the cells from differentiating, at least at a gross level. Another method for testing the developmental potential of ESCs is assessing the formation of beating clusters of cardiac cells. For this assay, cells are differentiated in hanging drops and then plated in individual wells to form a monolayer in differentiation media. After 10–15 days of differentiation, each well is visually examined for the presence of pulsing cells. Beating clusters formed from both WT and mutant cells. There was some variation in the proportion of EBs that could form beating clusters between the two 681C mutant strains, but in all cases the mutant cells could form beating clusters (Fig. 2G). These data bolster the conclusion that the reduction in H3K27me3 does not prevent cells from differentiating. This phenotype raised the issue of whether there are molecular changes caused by the point mutation.

Molecular phenotype of *Ezh2* point-mutant cells

To determine whether there were molecular phenotypes associated with the hypomorphic mutation of *Ezh2*, and the resultant loss of H3K27me3, we determined the target genes of PRC2 in our cell lines and measured their gene expression levels. We performed CUT&RUN analysis using antibodies to H3K27me3, H3K27Ac, RING1b, EZH2 and SUZ12 in WT and point-mutant cells as ESCs and as EBs after differentiation for 8 days. There have only been a small number of studies of PRC2 localization in differentiating cells, but of the ~7000 target genes we identified as having an H3K27me3 peak within 1 kb of their transcription start site in WT cells, just over 70% overlapped with previously published data (Fig. 3A; Juan et al., 2016). We note that peaks called from our dataset that did not overlap with previously called peaks showed signal in the published data that was below the threshold, indicating further agreement between the analysis done here and previous work. The same held true for PRC2 component SUZ12 (Fig. S3C, D; Li et al., 2017). There were far more targets called using H3K27me3 than with the individual components of either Polycomb complex, though the targets are largely overlapping (Fig. 3B). This is likely owing to differences in the strength of individual antibodies. Therefore, we used the targets identified with H3K27me3 for further analysis. In keeping with the western blot from whole-cell lysates, H3K27me3 was reduced on target genes in mutant cells (Fig. 3C). Levels of H3K27me3 were significantly lower in mutant cells at day 4 of differentiation and then were increased at day 8 of differentiation but to levels well below WT levels. The residual trimethylation at day 8 might be due to EZH1 function (Lavarone et al., 2019; Margueron et al., 2008; Shen et al., 2008). We focus below on the events that happen during these first 4 days of differentiation and the impact of the lack of H3K27me3 during this time frame. We conclude that the ability of the mutant cells to differentiate was not due to retention of normal trimethylation levels specifically on target genes.

The experiments described above using small molecule inhibitors revealed that there are genes that require H3K27me3 for their regulation and those that do not require H3K27me3 to maintain proper regulation. We investigated whether the point-mutant cells showed these same two gene classes. We performed RNA-seq analysis from ESCs and both day 4 and day 8 EBs from WT, CJ7

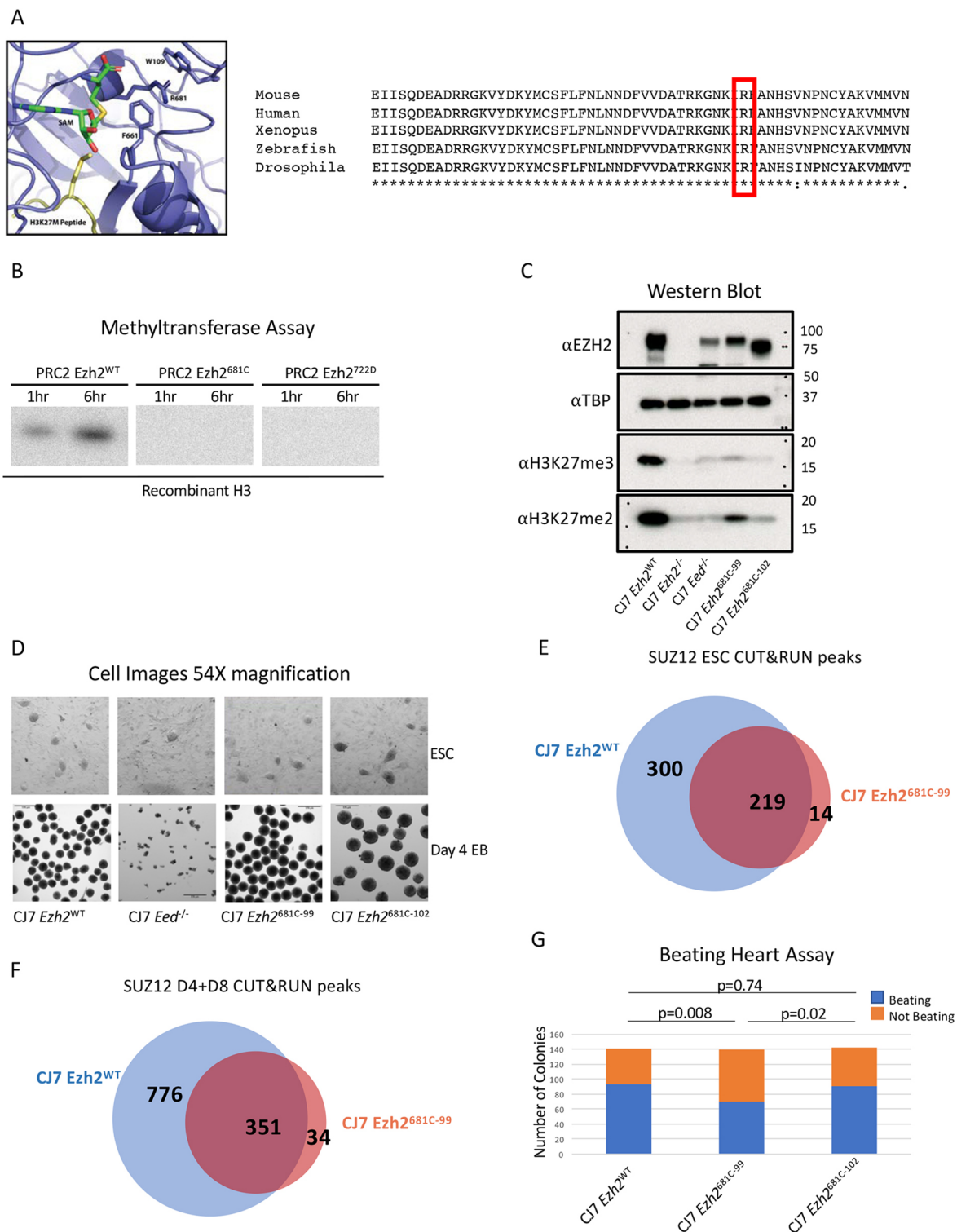


Fig. 2. Point mutation of a conserved residue within the SET domain inhibits methyltransferase activity. (A) Diagram of *Ezh2* SET domain structure with the 681 residue labeled. The SAM methyl donor is in green and the H3K27 M peptide is in yellow. An alignment of *Ezh2* SET domains with the analogous residue is highlighted in red. It is highly conserved across species (right). (B) *In vitro* methyltransferase assay with PRC2 comprising WT or mutant EZH2, EED, SUZ12 and AEBP2. Recombinant H3 is the substrate and a radioactive SAM was the methyl donor. Reactions progressed for 1 or 6 h. (C) Western blot from WT, mutant and PRC2 knockout cells probed with H3K27me, EZH2 and control TBP antibodies. (D) Representative images showing 54× magnification of embryonic stem cells (ESCs) or of embryoid bodies (EBs) that have differentiated for 4 days from WT, 681C-99, 681C-102 and *Eed*^{-/-} cells. (E) Venn diagram showing the overlap in CUT&RUN SUZ12 peaks between WT and 681C-99 mutant ESCs. (F) Venn diagram showing the overlap in CUT&RUN SUZ12 peaks between WT and 681C-99 mutant differentiated cells. (G) Quantification of beating heart assay from WT, 681C-99 and 681C-102 cells that were differentiated as EBs for 4 days and then individually plated in differentiation media. Blue shows the number of EBs that gave rise to beating cells and orange shows those that did not. For each cell type, 140 individual EBs were differentiated. *P*-values were calculated using a two proportion z-test.

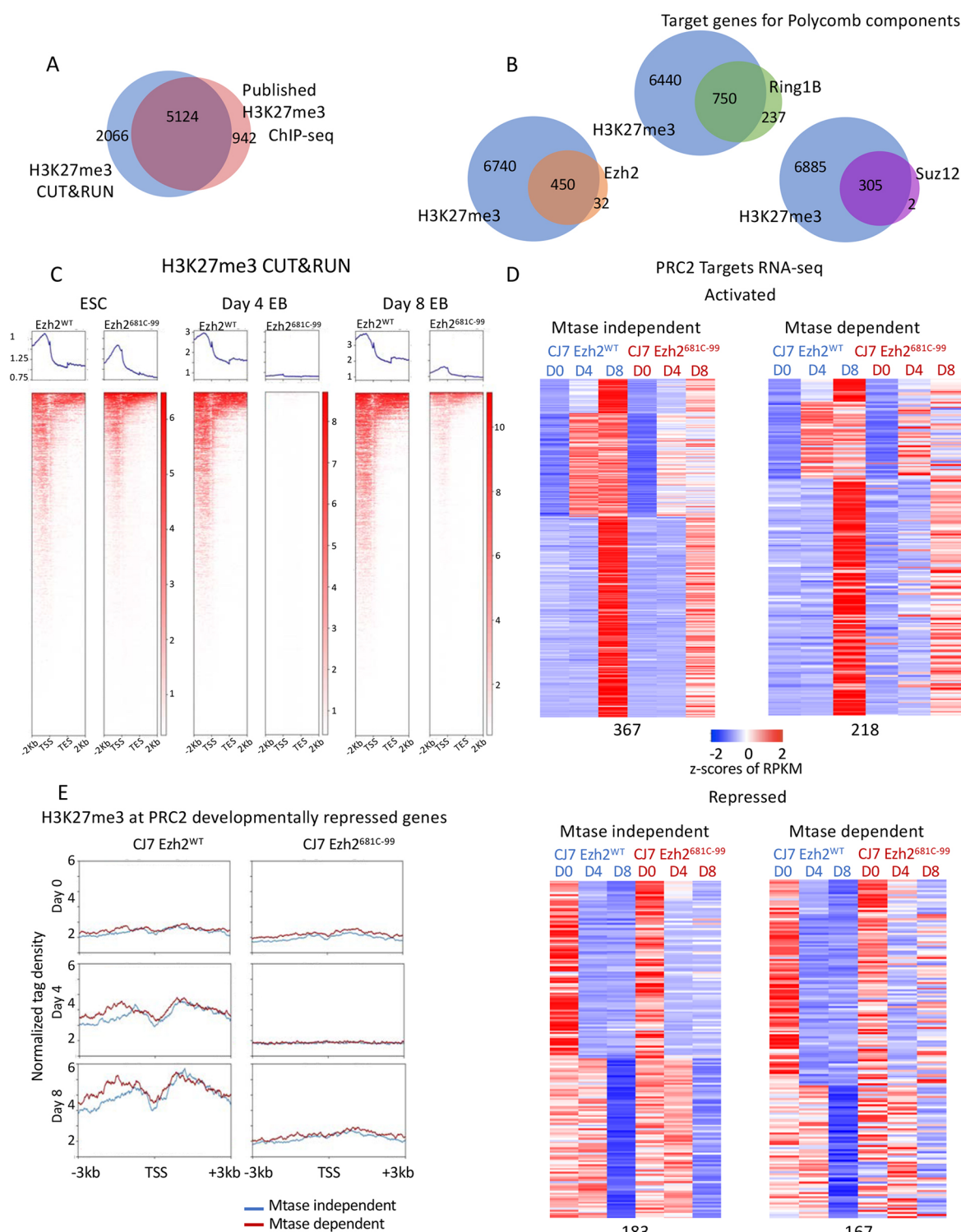


Fig. 3. The 681C point mutant shows reduced H3K27me3 on target genes regardless of whether they are dependent on the modification for normal expression. (A) Venn diagram showing overlap of H3K27me3 CUT&RUN and published ChIP-seq data peaks. (B) Venn diagrams showing overlap of target genes of H3K27me3 and other PRC2 components by CUT&RUN. (C) Average profiles and individual gene profiles of 7190 PRC2 target genes showing H3K27me3 CUT&RUN signal at day 0, 4 and 8 in WT and mutant cells. (D) Heatmap showing expression patterns of methyltransferase (Mtase)-dependent and -independent PRC2 target genes in WT and mutant ESCs over developmental time course. z-Scores of average RPKMs of triplicates are shown for each gene across all samples. Genes are separated based on whether they were activated (upper panels) or repressed (bottom panels) in WT cells over time as well as whether they had a similar expression pattern in mutant cells (Mtase-dependent genes; right) or a different expression pattern (Mtase-independent genes; left). The four groups are further clustered based on fold changes over time in untreated cells. All of the classifications were made based on a 1.5-fold change cutoff in expression levels over time. (E) Average profiles showing H3K27me3 enrichment in WT and mutant cells by CUT&RUN at Mtase-dependent (167) or -independent (183) and developmentally repressed PRC2 target genes over the time course.

Ezh2^{681C-99} and CJ7 Ezh2^{681C-102} cells. The data for both mutant cell lines nearly overlap and so for clarity we present the data from the CJ7 Ezh2^{681C-99} (Fig. S4). For this analysis, we defined PRC2 target genes as those that had a statistically significant peak of H3K27me3 from CUT&RUN at any time point in the EB formation protocol. PRC2 target genes were identified using WT H3K27me3 peaks called by Homer using a *P*-value threshold of 0.001, a length of at least 1500 bp, 1 read per kilo base per million mapped reads (RPKM) in at least two time points and signal overlapping Refseq annotated genes (TSS±5 kb). As with the cells treated with the small molecule inhibitor, we could separate genes that rely on H3K27me3 from those that do not need a high level of the modification for their regulation (Fig. 3D). The gene expression patterns from the mutant cells and the GSK343-treated cells clustered based upon day of differentiation rather than by whether they were drug treated or mutant (Fig. S5), although the correlation was not as strong as that seen between the two mutant cell lines. We detected both activated and repressed genes that fell into methyltransferase-dependent and -independent categories. The 350 genes that are normally repressed during differentiation in WT cells, and were either similarly repressed or were not repressed in mutant cells, showed more consistent patterns than the genes that were normally activated in WT cells. These patterns were well established by day 4 of differentiation, thus we used repressed genes to further analyze any characteristics specific to the methyltransferase-dependent or -independent genes.

We examined whether the level of H3K27me3 normally found on the genes in WT cells or the amount of signal remaining in the mutant cells could predict whether a gene would be dependent on the modification for its regulation. However, there was no difference in the levels of trimethylation based on whether the genes require this modification for their regulation (Fig. 3E). There was also strong overlap in the genes with PRC2 peaks, suggesting that the complex was still targeted normally (Fig. 2E,F). We then examined several characteristics of 350 genes that are normally repressed during differentiation of WT ESCs including other histone modifications, CpG methylation, and further sub-dividing genes by their dependence on H3K27me3 (Fig. S6). None of these characteristics showed any significant differences between genes with repression dependent upon methyltransferase activity and genes with repression not dependent on methyltransferase activity. We conclude that there is a variable reliance on H3K27me3 for gene regulation and that H3K27me3 is not the only driver of PRC2 target gene repression during EB formation, just as full levels are not needed for differentiation.

Methyltransferase point mutants cannot maintain differentiated cell identity

A major issue in developmental gene expression concerns the interplay between establishment and maintenance of gene expression profiles during differentiation. The Polycomb group (PcG) system, including PRC2, plays a role in both aspects of gene regulation in flies and in mammals. Substantial early work on mutant *Drosophila* highlighted a role for the PcG, including gene products now known to compose PRC2, in maintenance. Given that we saw limited impact of the ablation of H3K27me3 on establishment of the differentiated EB phenotype, we tested whether the mutant or drug-treated mouse cells were able to maintain a differentiated state.

Under normal conditions, cells differentiated into EBs cannot revert to ESCs without major manipulation such as introducing Yamanaka transcription factors (Nakagawa et al., 2008; Takahashi and Yamanaka, 2006). To determine whether the 681C point-mutant cells stably committed to a differentiated state, we formed day 8 EBs with WT and mutant cells, dissociated the EBs into single cells and re-plated them in ESC conditions without any additional manipulation. The cells were cultured in the ESC media for 5 days and then stained for alkaline phosphatase (AP) activity. After incubation with an appropriate colorimetric substrate, ESCs become bright pink owing to their AP activity, whereas feeder cells or any other differentiated cells remain unstained. We found a tenfold increase in the number of AP-positive colonies generated by the mutant cells over the WT (Fig. 4A,B). We asked whether this lack of commitment was maintained after longer periods of differentiation and found that after 14 days there remained more cells that could revert to ESCs, but to a considerably lesser extent than seen after 8 days (Fig. 4A,B). We conclude that the mutant cells are not stably committed to the more defined lineages but can switch back to an undifferentiated state, but that this flexibility decreases after 2 weeks of differentiation.

We used the small molecule inhibitor GSK343 to examine the time period during which this flexibility is established. There were three possibilities: (1) full levels of H3K27me3 might be needed continuously to maintain the differentiated state; (2) full levels of H3K27me3 might be needed at specific times as the cells are differentiating; (3) full levels of H3K27me3 might be needed only when cells are challenged with external stimuli that allow reversion to ESCs. Examination of the mutant cells addressed blocking full levels of methylation throughout the experimental time course, but did not address the time period when that lack of activity was most important. To separate the possibilities, we added or removed

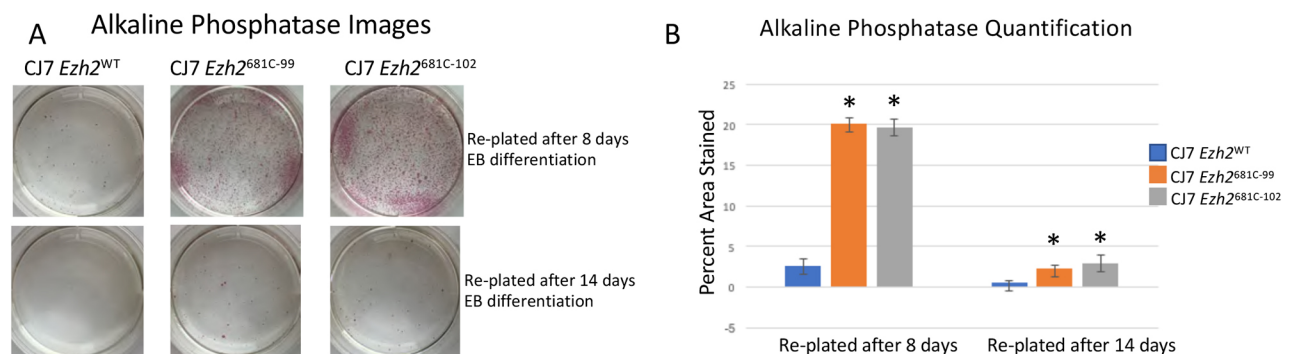


Fig. 4. Mutant cells are less stably differentiated than WT cells. (A) AP staining from WT, 681C-99 and 681C-102 cells that had been differentiated for 8 or 14 days and then transferred into ESC conditions for 5 days before staining. ESCs stain bright pink in this assay. (B) Quantification of AP staining from two biological replicates of re-plated cells. Data are mean±s.d. **P*<0.05 (unpaired two-tailed Student's *t*-test).

GSK343 during the differentiation time course (Fig. 5A shows the experimental design). To mimic the WT and point-mutant conditions a subset of cells were treated continuously with DMSO or GSK343 respectively. These treatments served as a baseline for altered times of GSK343 application. They also served to validate that the results observed with re-plating of mutant cells were not caused

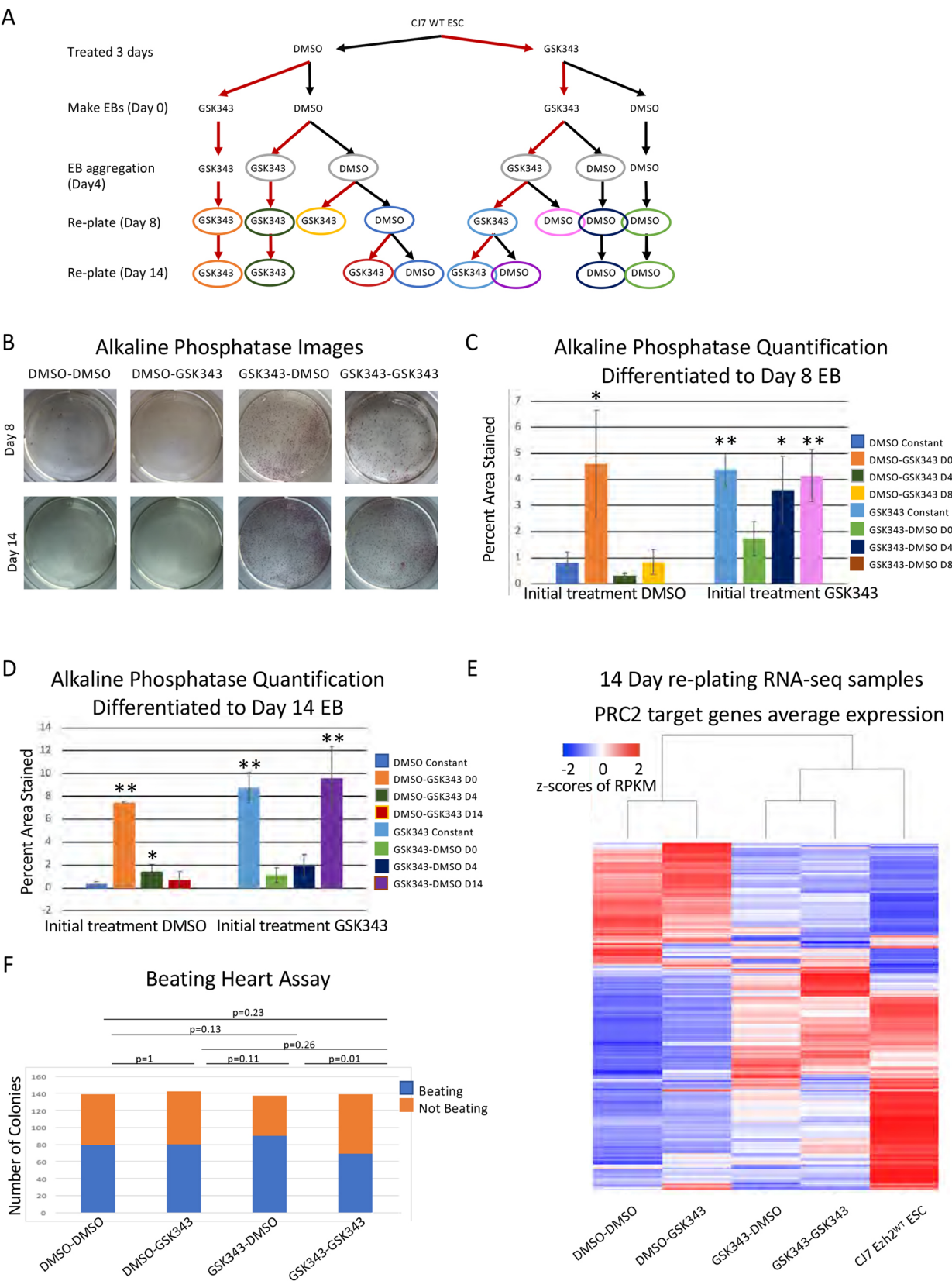


Fig. 5. See next page for legend.

Fig. 5. The crucial time period for H3K27me3 is within the first 4 days of differentiation. (A) Diagram showing the drug treatment plan for differentiation and re-plating of cells. Light gray circles indicate the cells used for the beating heart assay (F), other colors correspond to the bar charts quantifying AP staining (C,D). (B) Images of AP staining from DMSO- or GSK343-treated cells re-plated in ES conditions for 5 days after 8 or 14 days of EB differentiation. A greater proportion of cells that start in GSK343 treatment stain pink, indicating that the cells have reverted to an ESC phenotype. (C,D) Quantification of AP staining from cells treated with DMSO or GSK343 re-plated after 8 days (C) or 14 days (D) of EB differentiation performed in triplicate. Time of the treatment switch is indicated in the key and corresponds with colors in A. Data are mean \pm s.d. * P <0.05, ** P <0.005 (unpaired two-tailed Student's t -test). (E) Unsupervised clustering of RNA-seq average expression of cells re-plated for 5 days after 14 days of EB formation. Cells that were treated with GSK343 have gene expression profiles that cluster with average expression from WT ESCs. All 7190 PRC2 target genes are shown. (F) Quantification of beating heart assay with GSK343- and DMSO-treated cells. Cells were differentiated as EBs for 4 days and then plated into differentiation media. Blue indicates the number of EBs that formed beating cells and orange indicates the number that did not. P -values were calculated using a two proportion z-test.

by off-target effects of the CRISPR genetic manipulation or by mutations acquired during selection of these cells. Cells continuously treated with GSK343 had higher numbers of AP-positive cells following re-plating at 8 days, similar to the mutant cells; in contrast to the mutant cells, there were even more AP-positive cells following re-plating after 14 days of differentiation in GSK343. GSK343 treatment has more potent effects on dimethylation than the point mutation, which might account for the increased plasticity seen at later time points in drug-treated cells (Fig. S7A).

In addition to continual treatment with inhibitor, we varied the timing of GSK343 addition as depicted in Fig. 5A. Briefly, we treated ESCs for 3 days with either DMSO or GSK343 before starting the differentiation. When EB formation was initiated or at day 4 of differentiation we changed the treatment from DMSO to GSK343 (or vice versa) for half of the cells. We also switched the treatment at the time of re-plating into the ESC conditions at day 8. Finally, we allowed cells to differentiate to day 14 and switched treatment regimen (Fig. 5A). The treatment type was switched just once in each scheme so we could determine whether blocking the methylation of H3K27 at early or later stages of differentiation had the greatest effect. These experiments allowed us to determine whether reducing H3K27me3 has the greatest effect on cell identity when the cells are differentiating, when they are challenged by re-plating or throughout the differentiating time course.

We found that the crucial window for treatment with the inhibitor was early during EB formation (Fig. 5B,C,D). Increased staining by AP activity was seen in all cells that had initially been treated with inhibitor, regardless of when it was removed (Fig. 5C,D). Notably, treating with GSK343 for 3 days before inducing differentiation, then removing the inhibitor when differentiation was initiated, led to a significant increase in ESCs following re-plating at day 8. We saw increased staining in re-plated cells after both 8 and 14 days of differentiation when those cells were initially treated with DMSO and the inhibitor was added at the onset of differentiation (Fig. 5C,D). We saw no increase when GSK343 was added at day 4 and differentiation proceeded to day 8 (Fig. 5C), and a modest but significant increase when inhibitor was added at day 4 and cells were left to differentiate for 14 days (Fig. 5D). This latter increase was smaller than that seen when inhibitor was added at day 0 and cells were left to differentiate for 14 days. We conclude that the inhibition of methyltransferase activity either immediately before differentiation or early during the differentiation allows the cells to

remain in a more plastic state such that they can revert to a stem cell-like phenotype when placed in the proper growth conditions.

When we examined the ability of cells to form beating colonies after treatment with the small molecule we found no difference in the proportion of colonies that spontaneously started beating between any of the treatment groups (Fig. 5F). This is consistent with the data from the point-mutant cells, in which both WT and mutant cells could form beating colonies, and further indicates that there is no deficit in the ability of the cells to differentiate when H3K27 methylation is inhibited. Thus, as was seen with the comparison of WT with point-mutant cells, the obvious difference between DMSO and small molecule-treated cells occurred when cells were challenged to grow in the ESC culture conditions (Fig. 5B,C). We conclude that H3K27me3 methylation is more important in maintaining the differentiated state than in generating that state, and that the crucial time window occurs early in the differentiation process.

The GSK343-treated cells and the mutant cells both appeared to revert to a pluripotent state. To verify that these cells retained developmental potential, we re-differentiated these cells and determined whether they display the characteristic ability of ESCs to develop more committed cells. We used the re-plated cells from both 681C mutant cells and those treated with the inhibitor and attempted to make EBs. Both sets of re-plated cells were able to make EBs, which confirms that they have developmental potential (Fig. S7B).

To examine whether the reversion to a pluripotent state involved substantive changes in gene expression, as opposed to gene expression changes in a few key genes, we examined the genome-wide gene expression pattern of the reverted cells and compared those with ESCs. To examine the molecular phenotype of the re-plated cells, we isolated and sequenced RNA from drug-treated day-14 cells that were re-plated and had reverted to ESC phenotype. Unsupervised clustering showed that the average expression profiles of the cells that had been treated with GSK343, and therefore had much higher levels of reversion, were more like WT ESCs than the DMSO-treated and re-plated control cells (Fig. 5E). We conclude that the cells we see staining with AP in our re-plating assays are reverting to an ESC phenotype. We examined the subset of PRC2 target genes that are normally repressed during differentiation and found that many are reactivated when cells treated with GSK343 are re-plated. This differs from the genes that are reactivated in the cells initially treated with DMSO. The changes in gene expression observed following re-plating of cells treated with GSK343 were significantly different from the patterns observed after the re-plating of cells treated with DMSO (Fig. S7C,D). These expression pattern changes show the same response to the time of treatment with GSK343 as seen above; reversion to the WT pattern requires GSK343 treatment early in differentiation. From these data we conclude that, though all cells are placed under developmental stress when re-plated into ESC conditions, only those in which H3K27 methylation has been blocked revert to an ESC phenotype. This underlines the importance of H3K27me3 in establishing the heritable gene expression profile of differentiated lineages.

DISCUSSION

These studies offer two advances in understanding the role for methylation of H3K27 during differentiation of ESCs into EBs. First, many PRC2 targets continue to be regulated in a normal manner during the first 4 days of differentiation despite significantly reduced H3K27me3 levels on these targets (Fig. 3). Thus, H3K27me3 is not necessary for repression of a significant set of

PRC2 targets, indicating compensating mechanisms for repression of these genes. Second, although many PRC2 targets are dysregulated when H3K27me3 is blocked, we did not observe a significant impact on differentiation. In contrast, there was a large enhancement of the ability of differentiated cells to revert to a pluripotent phenotype when placed into ESC culture conditions. We conclude that the primary role for H3K27 methylation during early differentiation of EBs is maintenance of the differentiated state.

Differentiated WT cells are not generally capable of reverting to an ESC phenotype when their growth conditions are altered by a change in media. In normal cases, it takes the reactivation of key transcription factors to allow cells to return to that state. In contrast, *Ezh2* point-mutant cells and those that have been treated with a small molecule inhibitor readily revert to an ESC phenotype when placed into media that supports that type of growth. This was seen at both the cellular and molecular level. When we varied the time windows in which inhibitor was present, we found that the crucial window for normal H3K27me3 levels was between the start of differentiation through the first 4 days of EB formation. Not having the ability to add the trimethylation modification at those early stages of differentiation sets the stage for the cells to be able to revert to an ESC phenotype when challenged, even when H3K27me3 was restored later during EB formation. In the setting of the early stages of ESC differentiation into EBs, the H3K27me3 modification is acting analogously to a stopper on a swinging door. When the modification is present the door will only open one way and the cells cannot go backward, but removal of the modification enables the door to swing both ways, allowing cells to go back and forth between the differentiated and pluripotent state in response to external signals.

There are potential implications for these data in terms of the use of small molecule inhibitors in therapeutic situations. Multiple adult cell types have different requirements for PRC2 during their differentiation. Most relevant to the inhibition of PRC2 is the development of blood cells. PRC2 is required for the differentiation of blood stem cells, which is the site of some of the highest levels of PRC2 expression in healthy adult tissues. If the phenotypes that we have observed during EB formation occur in a similar manner in blood stem cells, treating patients with the small molecule inhibitors might alter the stability of commitment of healthy stem cells, raising the possibility of novel cancers arising from cells that cannot stably differentiate. Indeed, at least one clinical trial was temporarily suspended because patients had developed novel cancers (Fioravanti et al., 2018; Harris, 2018; Italiano et al., 2018). Determining the effect of blocking H3K27me3 in other differentiating cell lineages might be important to clinical intervention by expanding the knowledge of the potential side effects.

We note that it is difficult to completely eliminate H3K27 methylation with mutations (Lavarone et al., 2019), and that the mutation we generated in *Ezh2* significantly reduces H3K27me3, especially early in differentiation, but does not eliminate all methylation of H3K27. This is both a limitation and an advantage; the significant impact on H3K27me3 early in differentiation allowed us to show that loss of trimethylation has a potent phenotype (unstable commitment) at this stage yet does not have a discernible differentiation phenotype. These data demonstrate a striking difference in the dependency of these two key phenotypes on H3K27me3. This *Ezh2* mutation also has a molecular phenotype when gene regulation is examined, raising the possibility that the network of genes that require H3K27me3 for appropriate regulation at this stage is primarily responsible for driving stable commitment to the differentiated state.

MATERIALS AND METHODS

Cell culture

ESCs

CJ7 WT, CJ7 *Ezh2*^{−/−} and CJ7 *Eed*^{−/−} cells were a generous gift from the laboratory of Stuart Orkin (Boston Children's Hospital and Harvard Medical School, USA). We cultured all ESCs on a monolayer of feeder mouse embryonic fibroblasts (MEFs) in ESC medium (DMEM, Gibco, 11995-506) supplemented with 20% fetal bovine serum (FBS), non-essential amino acid solution, penicillin/streptomycin (pen/strep), glutamax and leukemia inhibitory factor (LIF) on tissue culture-treated flasks coated with 0.2% gelatin. The medium was changed daily and cells were split every 2-3 days.

EZH2 point-mutant cells

Point mutations were introduced into CJ7 WT using CRISPR RNP transfected into cells with the Amara mouse ES kit (Lonza, VPH-1001). Then 1×10⁶ cells were transfected with the RNP containing two separate guide RNAs, a single-stranded donor oligo and a linearized puromycin resistance gene. Cells were plated into three wells of a six-well plate with puroR MEFs and regular ESC medium. The next day, puromycin was added to the wells in a range of concentrations and kept on the cells for the next 2 days. Following selection, resistant cells were expanded, individual colonies were then re-plated into 24-well plates and checked for the presence of the mutation by restriction enzyme digestion followed by confirmation with sequencing. All cells were periodically monitored for mycoplasma contamination via PCR.

EB formation

EBs were formed using the hanging drop method (Behringer et al., 2016; Dang et al., 2002). Briefly, ESCs were trypsinized, de-MEFed and then resuspended in differentiation media (IMDM, Gibco, 12440-053) supplemented with 20% FBS, pen/strep and glutamax; no LIF). Droplets containing ~180 cells were incubated for 4 days so that spheres of differentiating cells could form. After the 4 days, EBs were collected and grown in suspension in non-adherent plates or used for subsequent experiments.

Beating heart assay

Beating clusters were differentiated from day 4 EBs (Boheler et al., 2002; Hescheler et al., 1997). Individual EBs were transferred into individual wells of a gelatinized 12-well plate. Cells were maintained in differentiation media throughout the experiment. Wells were monitored for beating colonies for the next 15 days and were scored as positive if there were any beating cells in that time period.

Western blot

The antibodies that were used to probe the western blots were: H3K27me3 (9733S, Cell Signaling Technology, 1:1000), H3K27me2 (9728S, Cell Signaling Technology, 1:5000) EZH2 (07-689, EMD Millipore, 1:15,000) and TBP (ab818, Abcam, 1:1000).

RNA-seq

RNA was isolated from whole cells using the Nucleospin RNA kit from Macherey Nagel (740955.50). We then depleted rRNA using the Ribozero Gold kit from Epicentre (RZG1224). cDNA was synthesized from the purified RNA using the Superscript Vilo cDNA sequencing kit from Thermo Fisher Scientific (11754050) and the libraries were assembled as previously described (Bowman et al., 2013). Three replicates were completed for all experimental conditions except the day 14 re-plated cells, for which two replicates were completed.

Methyltransferase assay

Purified protein complexes were incubated at room temperature with a histone substrate at a final concentration of 500 nM and ~500 nM radioactive SAM (adenosyl-L-methionine, S-methyl³H, PerkinElmer, NET155H250UC) in methyltransferase buffer [10% glycerol, 25 mM HEPES (pH 7.9), 2 mM MgCl₂ with 1 mM DTT added fresh]. Unless otherwise specified all reactions ran for 1 h before being stopped with the

addition of 6× SDS buffer. Samples were then run on an SDS PAGE gel, Coomassie stained and incubated in AMPLIFY (Amersham/GE, NAMP100) for 20 min. The gel was dried and exposed to film for a minimum of 24 h before developing.

Protein purification

The open reading frame for each member of the core PRC2 complex was cloned into the pFastBac1 baculovirus with Suz12 tagged with 3×Flag. Sf9 transfection with bacmid DNA and virus amplification were performed essentially as described for the Bac-to-Bac Baculovirus Expression System (Thermo Fisher Scientific). Sf9 cells were maintained in Hyclone CCM3 (CCM3 liquid medium with L-glutamine, GE Healthcare Life Sciences SH30065.02) supplemented with 50 U/ml pen/strep (Thermo Fisher Scientific, 15140-122). For protein expression, 2×10⁶ Sf9 cells/ml were infected at a multiplicity of infection of ~10. Cells were harvested 66 h post infection by centrifugation at 5000 g for 15 min. Cells were lysed, treated with DNaseI then the complex was bound to M2 and the complex was eluted with flag peptide.

CUT&RUN

CUT&RUN experiments were performed as previously described (Skene and Henikoff, 2017). The antibodies used were: H3K27me3 (9733S, Cell Signaling Technology, 1:100), EZH2 (5246S, Cell Signaling Technology, 1:100), SUZ12 (3737S, Cell Signaling Technology, 1:100) and RING1b (A302-869A, Bethyl Laboratories, 1:100). Libraries were constructed as described in the RNA-seq section. Two replicates were completed and representative experiments are shown.

AP assay

Cells were stained according to the instructions in the Stemgent AP Staining Kit II from Reprocell (00-0055). Images of stained wells were quantified using ImageJ FIJI software.

Bioinformatics methods

All RNA-seq reads were aligned to the mm10 genome using STAR v2.5.3 (Dobin et al., 2013). Gene annotations were obtained from Ensembl (Hunt et al., 2018). Genome browser tracks were generated using Homer v4.10.3 (Heinz et al., 2010) and visualized in IGV (Robinson et al., 2011). Reads in exons of Refseq annotated genes were counted using featureCounts v1.6.1 (Liao et al., 2014). edgeR (Robinson et al., 2010) was used to normalize reads and calculate false discovery rate (FDR) using triplicates. All further calculations and figures were made using R v3.3.2 (Dessau and Pipper, 2008). For all heatmaps, standard z-scores calculations were made using average RPKMs of triplicates for each gene across all conditions. Genes were narrowed down to only PRC2 targets using H3K27me3 CUT&RUN data. Only genes changing in untreated or WT cells over the time course were used for further analysis. The genes were filtered using cut-offs of at least 0.5 RPKM average expression at any time point, at least 1.5-fold change and maximum 0.05 FDR while comparing day 8 and day 4 or day 4 and day 0. Genes were then clustered based on up- or downregulation in control cells and up- or downregulation or unchanged gene expression in mutant or treated cells.

For Fig. 5E, unsupervised clustering was performed using R's heatmap.2 function. CpG and GC levels were calculated using Homer's annotatePeaks function.

All CUT&RUN reads were aligned to the mm10 genome using bowtie2 and filtered using samtools (Li et al., 2009) to keep uniquely aligned reads. Genome browser tracks were generated using Homer v4.10.3 and visualized in IGV. Peaks were called using the Homer findPeaks function for broad peaks. PRC2 target genes were identified using WT H3K27me3 peaks at least 1500 bp in length, 1 RPKM in at least two time points and overlapping Refseq annotated genes (TSS+/-5 kb). DeepTools v3.3.0 (Ramírez et al., 2014) was used to make average profile plots for Fig. 3E.

Published data for other canonical and non-canonical PRC2 components was downloaded from GEO as follows: H3K27me3 (GSM2282188, GSM2282191, GSM2282192) (Juan et al., 2016), SUZ12 (GSE97805)

(Li et al., 2017), EPOP (GSM2098943) (Beringer et al., 2016), Jarid2 (GSM491760) (Li et al., 2010), H3K4me1 (GSM1180178), H3K4me3 (GSM1180179), H3K9me3 (GSM1180180), H3K36me3 (GSM1180183) (Hon et al., 2014). FASTQ files were downloaded from GEO using sratools v2.9.1 (<https://ncbi.github.io/sra-tools/>). All reads were aligned to the mm10 genome using bowtie2 and filtered using samtools to keep uniquely aligned reads. Genome browser tracks were generated using Homer v4.10.3. DeepTools v3.3.0 was used to make average profile plots for Fig. 3C,E. Line plots were generated using R.

Acknowledgements

We thank Dr Jesse Cochrane for assistance in creating Fig. 2A and Dr Elizabeth Jaensch and Dr Christos Tsokos for critical reading of the manuscript. We also thank the lab of Dr Stuart Orkin for the gift of Cj7 WT, Ezh2^{-/-} and Eed^{-/-} ESCs.

Competing interests

The authors declare no competing or financial interests.

Author contributions

Conceptualization: S.A.M., R.E.K.; Software: M.D.; Validation: S.A.M.; Formal analysis: S.A.M., M.D.; Investigation: S.A.M., J.K.; Resources: R.E.K.; Data curation: M.D.; Writing - original draft: S.A.M., R.E.K.; Writing - review & editing: S.A.M., M.D., J.K., R.E.K.; Visualization: S.A.M., M.D.; Supervision: R.E.K.; Funding acquisition: R.E.K.

Funding

This work was supported by the National Institutes of Health [R35-GM131743 and R37-GM048405 to R.E.K.] and by the Urology Care Foundation Research Scholar Award Program [2018A012748 to J.K.]. Deposited in PMC for release after 12 months.

Data availability

All sequencing data have been deposited in the NCBI GEO database under the accession number GSE151486.

Supplementary information

Supplementary information available online at <https://dev.biologists.org/lookup/doi/10.1242/dev.196329.supplemental>

Peer review history

The peer review history is available online at <https://journals.biologists.com/dev/article-lookup/148/7/dev196329/>

References

- Abdel Raouf, S. M., Ibrahim, T. R., Abdelaziz, L. A., Farid, M. I. and Mohamed, S. Y. (2021). Prognostic value of TWIST1 and EZH2 expression in colon cancer. *J. Gastrointest. Cancer* **52**, 90-98. doi:10.1007/s12029-019-00344-4
- Ahmed, A., Wang, T. and Delgado-Olguin, P. (2018). Ezh2 is not required for cardiac regeneration in neonatal mice. *PLoS ONE* **13**, e0192238. doi:10.1371/journal.pone.0192238
- Aloia, L., Di Stefano, B. and Di Croce, L. (2013). Polycomb complexes in stem cells and embryonic development. *Development* **140**, 2525-2534. doi:10.1242/dev.091553
- Antonyasamy, S., Condon, B., Druzina, Z., Bonanno, J. B., Gheyi, T., Zhang, F., MacEwan, I., Zhang, A., Ashok, S., Rodgers, L. et al. (2013). Structural context of disease-associated mutations and putative mechanism of autoinhibition revealed by X-ray crystallographic analysis of the EZH2-SET domain. *PLoS ONE* **8**, e84147. doi:10.1371/journal.pone.0084147
- Basheer, F., Giotopoulos, G., Meduri, E., Yun, H., Mazan, M., Sasca, D., Gallipoli, P., Marando, L., Gozdecka, M., Asby, R. et al. (2019). Contrasting requirements during disease evolution identify EZH2 as a therapeutic target in AML. *J. Exp. Med.* **216**, 966-981. doi:10.1084/jem.20181276
- Behringer, R., Gertsenstein, M., Nagy, K. V. and Nagy, A. (2016). Differentiating mouse embryonic stem cells into embryoid bodies by hanging-drop cultures. *Cold Spring Harb. Protoc.* **2016**, 1073-1076. doi:10.1101/pdb.prot092429
- Beringer, M., Pisano, P., Di Carlo, V., Blanco, E., Chammas, P., Vizán, P., Gutiérrez, A., Aranda, S., Payer, B., Wierer, M. et al. (2016). EPOP Functionally links elongin and polycomb in pluripotent stem cells. *Mol. Cell* **64**, 645-658. doi:10.1016/j.molcel.2016.10.018
- Bernstein, E., Duncan, E. M., Masui, O., Gil, J., Heard, E. and Allis, C. D. (2006). Mouse polycomb proteins bind differentially to methylated histone H3 and RNA and are enriched in facultative heterochromatin. *Mol. Cell. Biol.* **26**, 2560-2569. doi:10.1128/MCB.26.7.2560-2569.2006

- Boheler, K. R., Czyz, J., Tweedie, D., Yang, H.-T., Anisimov, S. V. and Wobus, A. M. (2002). Differentiation of pluripotent embryonic stem cells into cardiomyocytes. *Circ. Res.* **91**, 189-201. doi:10.1161/01.RES.0000027865.61704.32
- Böhm, J., Muenzner, J. K., Caliskan, A., Ndrekhkja, B., Erlenbach-Wünsch, K., Merkel, S., Croner, R., Rau, T. T., Geppert, C. I., Hartmann, A. et al. (2019). Loss of enhancer of zeste homologue 2 (EZH2) at tumor invasion front is correlated with higher aggressiveness in colorectal cancer cells. *J. Cancer Res. Clin. Oncol.* **145**, 2227-2240. doi:10.1007/s00432-019-02977-1
- Bowman, S. K., Simon, M. D., Deaton, A. M., Tolstorukov, M., Borowsky, M. L. and Kingston, R. E. (2013). Multiplexed Illumina sequencing libraries from picogram quantities of DNA. *BMC Genomics* **14**, 466. doi:10.1186/1471-2164-14-466
- Bradley, W. D., Arora, S., Busby, J., Balasubramanian, S., Gehling, V. S., Nasveschuk, C. G., Vaswani, R. G., Yuan, C.-C., Hatton, C., Zhao, F. et al. (2014). EZH2 inhibitor efficacy in non-Hodgkin's lymphoma does not require suppression of H3K27 monomethylation. *Chem. Biol.* **21**, 1463-1475. doi:10.1016/j.chembiol.2014.09.017
- Bremer, S. C. B., Conradi, L.-C., Mechie, N.-C., Amanzada, A., Mavropoulou, E., Kitz, J., Ghadimi, M., Ellenrieder, V., Ströbel, P., Hessmann, E. et al. (2021). Enhancer of Zeste Homolog 2 in colorectal cancer development and progression. *Digestion* **102**, 227-235. doi:10.1159/000504093
- Chamberlain, S. J., Yee, D. and Magnuson, T. (2008). Polycomb repressive complex 2 is dispensable for maintenance of embryonic stem cell pluripotency. *Stem Cells* **26**, 1496-1505. doi:10.1634/stemcells.2008-0102
- Collinson, A., Collier, A. J., Morgan, N. P., Sienerth, A. R., Chandra, T., Andrews, S. and Rugg-Gunn, P. J. (2016). Deletion of the Polycomb-group protein EZH2 leads to compromised self-renewal and differentiation defects in human embryonic stem cells. *Cell Rep.* **17**, 2700-2714. doi:10.1016/j.celrep.2016.11.032
- Cyrus, S., Burkhardt, D., Weaver, D. D. and Gibson, W. T. (2019). PRC2-complex related dysfunction in overgrowth syndromes: a review of EZH2, EED, and SUZ12 and their syndromic phenotypes. *Am. J. Med. Genet. C Semin. Med. Genet.* **181**, 519-531. doi:10.1002/ajmg.c.31754
- Dang, S. M., Kyba, M., Perlingeiro, R., Daley, G. Q. and Zandstra, P. W. (2002). Efficiency of embryoid body formation and hematopoietic development from embryonic stem cells in different culture systems. *Biotechnol. Bioeng.* **78**, 442-453. doi:10.1002/bit.10220
- Deng, Y., Chen, X., Huang, C., Chen, G., Chen, F., Lu, J., Shi, X., He, C., Zeng, Z., Qiu, Y. et al. (2019). EZH2/Bcl-2 coexpression predicts worse survival in diffuse large B-cell lymphomas and demonstrates poor efficacy to rituximab in localized lesions. *J. Cancer* **10**, 2006-2017. doi:10.7150/jca.29807
- Dessau, R. B. and Phipps, C. B. (2008). [“R”-project for statistical computing]. *Ugeskr. Laeger.* **170**, 328-330. (R-en programpakke til statistisk databehandling og grafik.).
- Dobin, A., Davis, C. A., Schlesinger, F., Drenkow, J., Zaleski, C., Jha, S., Batut, P., Chaisson, M. and Gingeras, T. R. (2013). STAR: ultrafast universal RNA-seq aligner. *Bioinformatics* **29**, 15-21. doi:10.1093/bioinformatics/bts635
- Dou, D., Ge, X., Wang, X., Xu, X., Zhang, Z., Seng, J., Cao, Z., Gu, Y. and Han, M. (2019). EZH2 contributes to cisplatin resistance in breast cancer by epigenetically suppressing miR-381 expression. *OncoTargets Ther.* **12**, 9627-9637. doi:10.2147/OTT.S214104
- Ferguson, J., Devarajan, M., DiNuoscio, G., Saiakhova, A., Liu, C.-F., Lefebvre, V., Scacheri, P. C. and Attit, R. P. (2018). PRC2 is dispensable in vivo for β -catenin-mediated repression of chondrogenesis in the mouse embryonic cranial mesenchyme. *G3* **8**, 491-503. doi:10.1534/g3.117.300311
- Fioravanti, R., Stazi, G., Zwergel, C., Valente, S. and Mai, A. (2018). Six years (2012-2018) of researches on catalytic EZH2 inhibitors: the boom of the 2-pyridone compounds. *Chem. Rec.* **18**, 1818-1832. doi:10.1002/tcr.201800091
- Franeau, S., Pali, C. G., McNeill, B., Ritso, M., Shelley, W. C., Prasain, N., Chu, A., Vion, E., Rieck, K., Nilufar, S. et al. (2017). Epigenetic activation of pro-angiogenic signaling pathways in human endothelial progenitors increases vasculogenesis. *Stem Cell Rep.* **9**, 1573-1587. doi:10.1016/j.stemcr.2017.09.009
- Harris, J. (2018). Partial clinical hold on tazemetostat trials lifted by FDA [News article]. *Targeted Oncol.* <https://www.targetedonc.com/view/partial-clinical-hold-on-tazemetostat-trials-lifted-by-fda>
- Healy, E., Mucha, M., Glancy, E., Fitzpatrick, D. J., Conway, E., Neikes, H. K., Monger, C., Van Mierlo, G., Baltissen, M. P., Koseki, Y. et al. (2019). PRC2.1 and PRC2.2 Synergize to Coordinate H3K27 Trimethylation. *Mol. Cell* **76**, 437-452.e6. doi:10.1016/j.molcel.2019.08.012
- Heinz, S., Benner, C., Spann, N., Bertolino, E., Lin, Y. C., Laslo, P., Cheng, J. X., Murre, C., Singh, H. and Glass, C. K. (2010). Simple combinations of lineage-determining transcription factors prime cis-regulatory elements required for macrophage and B cell identities. *Mol. Cell* **38**, 576-589. doi:10.1016/j.molcel.2010.05.004
- Hescheler, J., Fleischmann, B. K., Lentini, S., Maltsev, V. A., Rohwedel, J., Wobus, A. M. and Addicks, K. (1997). Embryonic stem cells: a model to study structural and functional properties in cardiomyogenesis. *Cardiovasc. Res.* **36**, 149-162. doi:10.1016/S0008-6363(97)00193-4
- Hon, G. C., Song, C.-X., Du, T., Jin, F., Selvaraj, S., Lee, A. Y., Yen, C.-A., Ye, Z., Mao, S.-Q., Wang, B.-A. et al. (2014). 5mC oxidation by Tet2 modulates enhancer activity and timing of transcriptome reprogramming during differentiation. *Mol. Cell* **56**, 286-297. doi:10.1016/j.molcel.2014.08.026
- Hunt, S. E., McLaren, W., Gil, L., Thormann, A., Schuilenburg, H., Sheppard, D., Parton, A., Armean, I. M., Trevanion, S. J., Flícek, P. et al. (2018). Ensembl variation resources. *Database* **2018**, bay119. doi:10.1093/database/bay119
- Italiano, A., Soria, J.-C., Toulmonde, M., Michot, J.-M., Lucchesi, C., Varga, A., Coindre, J.-M., Blakemore, S. J., Clawson, A., Suttle, B. et al. (2018). Tazemetostat, an EZH2 inhibitor, in relapsed or refractory B-cell non-Hodgkin lymphoma and advanced solid tumours: a first-in-human, open-label, phase 1 study. *Lancet Oncol.* **19**, 649-659. doi:10.1016/S1470-2045(18)30145-1
- Jain, P. and Di Croce, L. (2016). Mutations and deletions of PRC2 in prostate cancer. *BioEssays* **38**, 446-454. doi:10.1002/bies.201500162
- Jiao, L. and Liu, X. (2015). Structural basis of histone H3K27 trimethylation by an active polycomb repressive complex 2. *Science* **350**, aac4383. doi:10.1126/science.aac4383
- Juan, A. H., Wang, S., Ko, K. D., Zare, H., Tsai, P.-F., Feng, X., Vivanco, K. O., Ascoli, A. M., Gutierrez-Cruz, G., Krebs, J. et al. (2016). Roles of H3K27me2 and H3K27me3 examined during fate specification of embryonic stem cells. *Cell Rep.* **17**, 1369-1382. doi:10.1016/j.celrep.2016.09.087
- Karlowee, V., Amatya, V. J., Takayasu, T., Takano, M., Yonezawa, U., Takeshima, Y., Sugiyama, K., Kurisu, K. and Yamasaki, F. (2019). Immunostaining of increased expression of enhancer of Zeste Homolog 2 (EZH2) in diffuse midline glioma H3K27M-mutant patients with poor survival. *Pathobiology* **86**, 152-161. doi:10.1159/000496691
- Kondo, Y. (2014). Targeting histone methyltransferase EZH2 as cancer treatment. *J. Biochem.* **156**, 249-257. doi:10.1093/jb/mvu054
- Krill, L., Deng, W., Eskander, R., Mutch, D., Zweig, S., Hoang, B., Ioffe, O., Randall, L., Lankes, H., Miller, D. S. et al. (2020). Overexpression of enhancer of Zeste homolog 2 (EZH2) in endometrial carcinoma: an NRG oncology/gynecologic oncology group study. *Gynecol. Oncol.* **156**, 423-429. doi:10.1016/j.ygyno.2019.12.003
- Lavarone, E., Barbieri, C. M. and Pasini, D. (2019). Dissecting the role of H3K27 acetylation and methylation in PRC2 mediated control of cellular identity. *Nat. Commun.* **10**, 1679. doi:10.1038/s41467-019-09624-w
- Lewis, E. and Mislove, R. (1947). New mutants report. *Drosoph. Inf. Serv.* **21**, 69.
- Li, H., Handsaker, B., Wysoker, A., Fennell, T., Ruan, J., Homer, N., Marth, G., Abecasis, G. and Durbin, R. (2009). The Sequence Alignment/Map format and SAMtools. *Bioinformatics* **25**, 2078-2079. doi:10.1093/bioinformatics/btp352
- Li, G., Margueron, R., Ku, M., Chambon, P., Bernstein, B. E. and Reinberg, D. (2010). Jarid2 and PRC2, partners in regulating gene expression. *Genes Dev.* **24**, 368-380. doi:10.1101/gad.1886410
- Li, H., Liefke, R., Jiang, J., Kurland, J. V., Tian, W., Deng, P., Zhang, W., He, Q., Patel, D. J., Bulys, M. L. et al. (2017). Polycomb-like proteins link the PRC2 complex to CpG islands. *Nature* **549**, 287-291. doi:10.1038/nature23881
- Liao, Y., Smyth, G. K. and Shi, W. (2014). featureCounts: an efficient general purpose program for assigning sequence reads to genomic features. *Bioinformatics* **30**, 923-930. doi:10.1093/bioinformatics/btt656
- Liu, T.-P., Lo, H.-L., Wei, L.-S., Hsiao, H.-H. and Yang, P.-M. (2015). S-Adenosyl-L-methionine-competitive inhibitors of the histone methyltransferase EZH2 induce autophagy and enhance drug sensitivity in cancer cells. *Anticancer Drugs* **26**, 139-147. doi:10.1097/CAD.0000000000000166
- Lue, J. K. and Amengual, J. E. (2018). Emerging EZH2 inhibitors and their application in lymphoma. *Curr. Hematol. Malig. Rep.* **13**, 369-382. doi:10.1007/s11899-018-0466-6
- Margueron, R. and Reinberg, D. (2011). The polycomb complex PRC2 and its mark in life. *Nature* **469**, 343-349. doi:10.1038/nature09784
- Margueron, R., Li, G., Sarma, K., Blais, A., Zavadil, J., Woodcock, C. L., Dynlacht, B. D. and Reinberg, D. (2008). Ezh1 and Ezh2 maintain repressive chromatin through different mechanisms. *Mol. Cell* **32**, 503-518. doi:10.1016/j.molcel.2008.11.004
- Matsubara, T., Toyokawa, G., Takada, K., Kinoshita, F., Kozuma, Y., Akamine, T., Shimokawa, M., Haro, A., Osoegawa, A., Tagawa, T. et al. (2019). The association and prognostic impact of enhancer of zeste homologue 2 expression and epithelial-mesenchymal transition in resected lung adenocarcinoma. *PLoS ONE* **14**, e0215103. doi:10.1371/journal.pone.0215103
- Mechaal, A., Menif, S., Abbes, S. and Safra, I. (2019). EZH2, new diagnosis and prognosis marker in acute myeloid leukemia patients. *Adv. Med. Sci.* **64**, 395-401. doi:10.1016/j.advms.2019.07.002
- Müller, J., Hart, C. M., Francis, N. J., Vargas, M. L., Sengupta, A., Wild, B., Miller, E. L., O'Connor, M. B., Kingston, R. E. and Simon, J. A. (2002). Histone methyltransferase activity of a *Drosophila* polycomb group repressor complex. *Cell* **111**, 197-208. doi:10.1016/S0092-8674(02)00976-5
- Nakagawa, M., Koyanagi, M., Tanabe, K., Takahashi, K., Ichisaka, T., Aoi, T., Okita, K., Mochizuki, Y., Takizawa, N. and Yamanaka, S. (2008). Generation of induced pluripotent stem cells without Myc from mouse and human fibroblasts. *Nat. Biotechnol.* **26**, 101-106. doi:10.1038/nbt1374
- O'Carroll, D., Erhardt, S., Pagani, M., Barton, S. C., Surani, M. A. and Jenuwein, T. (2001). The polycomb-group geneEzh2 is required for early mouse development. *Mol. Cell. Biol.* **21**, 4330-4336. doi:10.1128/MCB.21.13.4330-4336.2001

- O'Geen, H., Ren, C., Nicolet, C. M., Perez, A. A., Halmaj, J., Le, V. M., Mackay, J. P., Farnham, P. J. and Segal, D. J. (2017). dCas9-based epigenome editing suggests acquisition of histone methylation is not sufficient for target gene repression. *Nucleic Acids Res.* **45**, 9901-9916. doi:10.1093/nar/gkx578
- Pasini, D., Bracken, A. P., Jensen, M. R., Denchi, E. L. and Helin, K. (2004). Suz12 is essential for mouse development and for EZH2 histone methyltransferase activity. *EMBO J.* **23**, 4061-4071. doi:10.1038/sj.emboj.7600402
- Pasini, D., Bracken, A. P., Hansen, J. B., Capillo, M. and Helin, K. (2007). The polycomb group protein Suz12 is required for embryonic stem cell differentiation. *Mol. Cell. Biol.* **27**, 3769-3779. doi:10.1128/MCB.01432-06
- Qi, W., Chan, H., Teng, L., Li, L., Chuai, S., Zhang, R., Zeng, J., Li, M., Fan, H., Lin, Y. et al. (2012). Selective inhibition of Ezh2 by a small molecule inhibitor blocks tumor cells proliferation. *Proc. Natl. Acad. Sci. USA* **109**, 21360-21365. doi:10.1073/pnas.1210371110
- Rai, A. N., Vargas, M. L., Wang, L., Andersen, E. F., Miller, E. L. and Simon, J. A. (2013). Elements of the polycomb repressor SU(Z)12 needed for histone H3-K27 methylation, the interface with E(Z), and in vivo function. *Mol. Cell. Biol.* **33**, 4844-4856. doi:10.1128/MCB.00307-13
- Ramírez, F., Dündar, F., Diehl, S., Grüning, B. A. and Manke, T. (2014). deepTools: a flexible platform for exploring deep-sequencing data. *Nucleic Acids Res.* **42**, W187-W191. doi:10.1093/nar/gku365
- Robinson, M. D., McCarthy, D. J. and Smyth, G. K. (2010). edgeR: a Bioconductor package for differential expression analysis of digital gene expression data. *Bioinformatics* **26**, 139-140. doi:10.1093/bioinformatics/btp616
- Robinson, J. T., Thorvaldsdóttir, H., Winckler, W., Guttman, M., Lander, E. S., Getz, G. and Mesirov, J. P. (2011). Integrative genomics viewer. *Nat. Biotechnol.* **29**, 24-26. doi:10.1038/nbt.1754
- Schuettengruber, B., Bourbon, H.-M., Di Croce, L. and Cavalli, G. (2017). Genome regulation by polycomb and Trithorax: 70 years and counting. *Cell* **171**, 34-57. doi:10.1016/j.cell.2017.08.002
- Shan, Y., Liang, Z., Xing, Q., Zhang, T., Wang, B., Tian, S., Huang, W., Zhang, Y., Yao, J., Zhu, Y. et al. (2017). PRC2 specifies ectoderm lineages and maintains pluripotency in primed but not naïve ESCs. *Nat. Commun.* **8**, 672. doi:10.1038/s41467-017-00668-4
- Shen, X., Liu, Y., Hsu, Y.-J., Fujiwara, Y., Kim, J., Mao, X., Yuan, G.-C. and Orkin, S. H. (2008). EZH1 mediates methylation on histone H3 lysine 27 and complements EZH2 in maintaining stem cell identity and executing pluripotency. *Mol. Cell* **32**, 491-502. doi:10.1016/j.molcel.2008.10.016
- Shen, X., Kim, W., Fujiwara, Y., Simon, M. D., Liu, Y., Mysliwiec, M. R., Yuan, G.-C., Lee, Y. and Orkin, S. H. (2009). Jumonji modulates polycomb activity and self-renewal versus differentiation of stem cells. *Cell* **139**, 1303-1314. doi:10.1016/j.cell.2009.12.003
- Shi, B., Behrens, C., Vaghani, V., Riquelme, E. M., Rodriguez-Canales, J., Kadara, H., Lin, H., Lee, J., Liu, H., Wistuba, I. et al. (2019). Oncogenic enhancer of zeste homolog 2 is an actionable target in patients with non-small cell lung cancer. *Cancer Med.* **8**, 6383-6392. doi:10.1002/cam4.1855
- Skene, P. J. and Henikoff, S. (2017). An efficient targeted nuclease strategy for high-resolution mapping of DNA binding sites. *eLife* **6**, e21856. doi:10.7554/eLife.21856
- Takahashi, K. and Yamanaka, S. (2006). Induction of pluripotent stem cells from mouse embryonic and adult fibroblast cultures by defined factors. *Cell* **126**, 663-676. doi:10.1016/j.cell.2006.07.024
- Thornton, S. R., Butty, V. L., Levine, S. S. and Boyer, L. A. (2014). Polycomb repressive complex 2 regulates lineage fidelity during embryonic stem cell differentiation. *PLoS ONE* **9**, e110498. doi:10.1371/journal.pone.0110498
- Tian, Z., Li, Z., Zhu, Y., Meng, L., Liu, F., Sang, M. and Wang, G. (2019). Hypermethylation-mediated inactivation of miR-124 predicts poor prognosis and promotes tumor growth at least partially through targeting EZH2/H3K27me3 in ESCC. *Clin. Exp. Metastasis* **36**, 381-391. doi:10.1007/s10585-019-09974-1
- van Mierlo, G., Veenstra, G. J. C., Vermeulen, M. and Marks, H. (2019). The complexity of PRC2 subcomplexes. *Trends Cell Biol.* **29**, 660-671. doi:10.1016/j.tcb.2019.05.004
- Wasenang, W., Puapairoj, A., Settassatian, C., Proungvitaya, S. and Limpaboon, T. (2019). Overexpression of polycomb repressive complex 2 key components EZH2/SUZ12/EED as an unfavorable prognostic marker in cholangiocarcinoma. *Pathol. Res. Pract.* **215**, 152451. doi:10.1016/j.prp.2019.152451
- Wassef, M., Luscan, A., Aflaki, S., Zielinski, D., Jansen, P. W. T. C., Baymaz, H. I., Battistella, A., Kersouani, C., Servant, N., Wallace, M. R. et al. (2019). EZH1/2 function mostly within canonical PRC2 and exhibit proliferation-dependent redundancy that shapes mutational signatures in cancer. *Proc. Natl. Acad. Sci. USA* **116**, 6075-6080. doi:10.1073/pnas.1814634116
- Wu, X., Scott, H., Carlsson, S. V., Sjöberg, D. D., Cerundolo, L., Lilja, H., Prevost, R., Rieunier, G., Macaulay, V., Higgins, G. S. et al. (2019). Increased EZH2 expression in prostate cancer is associated with metastatic recurrence following external beam radiotherapy. *Prostate* **79**, 1079-1089. doi:10.1002/pros.23817
- Xu, B., On, D. M., Ma, A., Parton, T., Konze, K. D., Pattenden, S. G., Allison, D. F., Cai, L., Rockowitz, S., Liu, S. et al. (2015). Selective inhibition of EZH2 and EZH1 enzymatic activity by a small molecule suppresses MLL-rearranged leukemia. *Blood* **125**, 346-357. doi:10.1182/blood-2014-06-581082
- Xu, H., Zhang, L., Qian, X., Zhou, X., Yan, Y., Zhou, J., Ge, W., Albahde, M. and Wang, W. (2019). GSK343 induces autophagy and downregulates the AKT/mTOR signaling pathway in pancreatic cancer cells. *Exp. Ther. Med.* **18**, 2608-2616. doi:10.3892/etm.2019.7845
- Yamagishi, M. and Uchimaru, K. (2017). Targeting EZH2 in cancer therapy. *Curr. Opin. Oncol.* **29**, 375-381. doi:10.1097/CCO.0000000000000390
- Yang, P. M., Hong, Y. H., Hsu, K. C. and Liu, T. P. (2019). p38 α /S1P/SREBP2 activation by the SAM-competitive EZH2 inhibitor GSK343 limits its anticancer activity but creates a druggable vulnerability in hepatocellular carcinoma. *Am. J. Cancer Res.* **9**, 2120-2139.
- Yu, W., Zhang, F., Wang, S., Fu, Y., Chen, J., Liang, X., Le, H., Pu, W. T. and Zhang, B. (2017). Depletion of polycomb repressive complex 2 core component EED impairs fetal hematopoiesis. *Cell Death Dis.* **8**, e2744. doi:10.1038/cddis.2017.163
- Zhang, M. J., Chen, D. S., Li, H., Liu, W. W., Han, G. Y. and Han, Y. F. (2019a). Clinical significance of USP7 and EZH2 in predicting prognosis of laryngeal squamous cell carcinoma and their possible functional mechanism. *Int. J. Clin. Exp. Pathol.* **12**, 2184-2194.
- Zhang, Q., Han, Q., Zi, J., Ma, J., Song, H., Tian, Y., McGrath, M., Song, C. and Ge, Z. (2019b). Mutations in EZH2 are associated with poor prognosis for patients with myeloid neoplasms. *Genes Dis.* **6**, 276-281. doi:10.1016/j.gendis.2019.05.001